Rational Design of Hybrid Graphene Films for High-Performance Transparent Electrodes

Yu Zhu, Zhengzong Sun, Zheng Yan, Zhong Jin, and James M. Tour*

Departments of Chemistry and Mechanical Engineering and Materials Science and the Smalley Institute for Nanoscale Science and Technology, Rice University, MS 222, 6100 Main Street, Houston, Texas 77005, United States

ABSTRACT Transparent, flexible conducting films were fabricated by using a metallic grid and graphene hybrid film. Transparent electrodes using the hybrid film and transparent substrate such as glass or polyethylene terephthalate (PET) films were assembled. The sheet resistance of the fabricated transparent electrodes was as low as 3 Ω/□ with the transmittance at ~80%. At 90% transmittance, the sheet resistance was ~20 Ω/□. Both values are among the highest for transparent electrode materials to date. The materials used for the new hybrid electrode are earth-abundant stable elements, which increase their potential usefulness for replacement of indium tin oxide (ITO) in many applications.

KEYWORDS: graphene · transparent electrode · metal grid · flexible

Transparent conducting films have been widely used in applications such as solar cells, light-emitting devices, and electronic touch screens. Theoretical and experimental[1−16] research indicates that graphene is a promising material for transparent electrodes. Monolayer graphene absorbs only 2.3% of visible light,[16] rendering it one of the most transparent conductors available. Experimental results have demonstrated that graphene has a 230 000 $cm^2\ V^{-1}\ s^{-1}$ electron mobility.[17] The resistivity of pristine graphene has been estimated to be as low as 10^{-6} Ω·cm,[18] which is a lower resistivity than silver. Generally the sheet resistance, R_s, is used to describe the electric conductivity of a two-dimensional transparent electrode. R_s has the following relationship to the mobility of materials:[19]

$$R_s = t/(qn_m\mu_m) \quad (1)$$

where n_m and μ_m are the majority carrier density and mobility respectively, q is the unit charge, and t is the thickness. On the basis of the experimental mobility data, monolayer graphene with a transmittance (T) of 97.7% will have a theoretical minimum sheet resistance of ~30 Ω/□[18] at a carrier density of 10^{12} cm^{-2}. This predicted value is better than the present commercial transparent conducting material, indium tin oxide (ITO), whose sheet resistance is typically ~30−80 Ω/□ when the T = 90%. However, graphene's extremely high mobility has only experimentally been observed on suspended graphene[17] that is produced from mechanical exfoliation of highly ordered pyrolytic graphite (HOPG).[17,20] Other scalable graphene-producing methods such as epitaxially grown graphene on silicon carbide[21] and chemical vapor deposited graphene on metals such as Ni[8,10,22] and Cu,[15] produce lower quality graphene. The highest mobility of synthesized graphene used in a large area transparent electrode is 5100 $cm^2\ V^{-1}\ s^{-1}$ at room temperature,[23] roughly 100× less than the highest reported mobility of mechanically exfoliated graphene.[17] Therefore, the typical experimental sheet resistance of undoped synthesized graphene is between 2k Ω/□ to 5k Ω/□ (also roughly 100× larger than the theoretical minimum).[10,15] For practical usage in transparent electrodes, a transmittance over 90% is required. This permits the assembly of up to four layers of graphene to reduce the sheet resistance while maintaining 90% transparency. However, the sheet resistance of four-layered undoped graphene is ~350 Ω/□,[7] thereby falling 10-fold short of the desired sheet resistance of monolayered graphene.

Since the mobility of the graphene is limited by the scalable production process, increasing the carrier density becomes an alternative method for reducing the sheet resistance of graphene. Various doping methods[6,23,24] have been suggested to make the graphene more conductive. As early as 2008, Blake *et al.*[6] demonstrated polyvinyl alcohol (PVA)-coated graphene exhibiting a sheet resistance of 450 Ω/□ due to the doping effect of PVA. Systematic

* Address correspondence to tour@rice.edu.

Received for review May 9, 2011 and accepted July 20, 2011.

Published online July 20, 2011
10.1021/nn201696g

studies have been reported recently for doped graphene-based transparent electrodes. Bae *et al.*[23] demonstrated that monolayer graphene doped by nitric acid exhibits a sheet resistance as low as 125 Ω/□ (T = 97%),[23] and the same four-layered graphene transparent electrode was reported with a sheet resistance of 30 Ω/□ (T = 90%).[23] Kim *et al.*[24] reported $AuCl_3$-doped graphene, which has a minimum sheet resistance of 150 Ω/□ (T = 87%).[24] Güneş *et al.*[25] proposed a method of layer-by-layer (LbL) doping of thin graphene films, which can reach a sheet resistance of 54 Ω/□ (T = 85%). In that work, graphene formed ion pairs with the dopant molecules. Although the performance of the transparent films produced using doped graphene have been similar to the performance of ITO, the stability of the graphene-dopant system is unknown. Similar doping effects have been studied in SWCNT films, and the doping enhancements had limited stability in air and under thermal loading.[26] Although an additional gas barrier layer might extend the lifetime of the chemically doped film, doped graphene might remain less stable than pristine graphene, and the fabrication cost would likely increase. Considering that a major application for transparent electrodes is in solar cells where the commercial product's lifetime is 25−30 years, and LED lamps having similar expected lifetimes, it is necessary to improve the graphene-based transparent electrode.

The practical limitations of the conventional methods for making graphene-based transparent electrodes can be overcome by assembling the transparent electrode in a way other than only using transparent materials. Instead, transparent electrodes can also be made using a nontransparent material such as metal nanowires[27−29] or carbon nanotubes.[2] Unlike transparent ITO, poly(3,4-ethylenedioxythiophene)/poly(styrenesulfonate) (PEDOT/PSS), and graphene, those materials themselves are opaque; however, they can form thin transparent percolation networks. The network can conduct current and leave large empty spaces that render these films transparent. On the basis of the understanding of these two approaches for making transparent conducting film, in this paper we disclose a graphene hybrid structure to reduce the sheet resistance of these synthetic graphene-based transparent electrodes, and even exceed the theoretical limit of a graphene film. The idea is to use a nontransparent, highly conductive metal to make the grid structure, and monolayer graphene is then transferred on top of the grid to fill the uncovered area (Figure 1).

The integration of the metal grid has many advantages. First, unlike graphene, which is a two-dimensional material, metal is a three-dimensional material. Although the resistivity of metal is higher than that of graphene,[18] it can have a smaller sheet resistance than monolayer graphene by using a thick film, based on

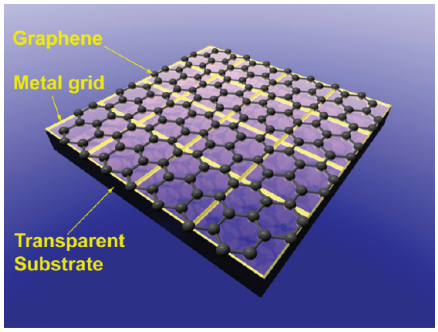

Figure 1. Metal grid/graphene hybrid transparent electrode. The yellow lines in the figure represent the metal grid. The grid size and gridline width in the figure are only illustrative and are not scaled with the graphene molecular structure.

the definition of sheet resistance:

$$R = (\rho/t)(L/W) = R_s(L/W) \quad (2)$$

Where R_s = sheet resistance, ρ = resistivity, R = resistance, t = thickness, W = width, L = length. A 100-nm silver film will have a sheet resistance of 0.16 Ω/□, *ca.* 200× smaller than the limited sheet resistance of graphene. Second, the graphene grown on copper or nickel substrates have inevitable defects induced by metal grain boundaries and the transferring techniques. For example, it is known that the grain size of crystalline copper is typically a few 100 μm and the defects have been found on the grain boundaries, which could be one reason for the high sheet resistance of synthesized graphene films[15,23] (see also Figure S1 in the Supporting Information). By using a suitable grid size (∼100 μm), the effects of those defects can be reduced (Supporting Information). Third, since monolayer graphene is almost transparent (it absorbs only 2.3% visible light), the transmittance of the hybrid film can be easily adjusted by modulating the metal grid size and gridline width. Lastly, the graphene film can be regarded as an enhancement to the grid-only structure as well. The metal grid-only structures used in this work, similar to nanotube and metal nanowire networks, are percolation-type electrodes. However, due to the size of the grid, they cannot be regarded as continuous electrodes for many applications. By applying a graphene overcoating to the metal grid structure, it is possible to make a continuous conducting film without increasing lithography cost.

The process sequence used in this work is as follows: the metal grids are first formed on the transparent substrate. Then, a graphene film is grown on a copper foil and isolated with a layer of sacrificial PMMA. The graphene film is transferred to the top of the grid and the sacrificial PMMA layer is removed to form the final hybrid transparent electrodes (see Methods and Scheme S1 in Supporting Information for detailed information). There are many ways to generate a metal grid structure on a transparent substrate. In this work, photolithography with wet-etching was applied to produce the metal grid structure (Methods). This procedure has the following advantages: First, photolithography is a

TABLE 1. Sheet Resistance and Transmittance of Graphene/Metal Grid Hybrid Films, Entries 1−10[a]

entry	name	grid size	grid line width	metal/substrate	sheet resistance (transmittance)[b] / sheet resistance without graphene
1	hybrid transparent conducting electrode	100 μm × 100 μm	10 μm	Au/glass	4 ± 1 Ω/□ (79%) /5 ± 1 Ω/□
2		200 μm × 200 μm	5 μm	Au/glass	20 ± 4 Ω/□ (91%) /22 ± 4 Ω/□
3		100 μm × 100 μm	10 μm	Al/glass	13 ± 2 Ω/□ (79%) /20 ± 4 Ω/□
4		200 μm × 200 μm	5 μm	Al/glass	45 ± 6 Ω/□ (91%) /52 ± 8 Ω/□
5		100 μm × 100 μm	10 μm	Cu/glass	3 ± 1 Ω/□ (79%) /4 ± 1 Ω/□
6		200 μm × 200 μm	5 μm	Cu/glass	22 ± 8 Ω/□ (91%) /26 ± 4 Ω/□
7		100 μm × 100 μm	10 μm	Al/PET	18 ± 9 Ω/□ (79%) /25 ± 6 Ω/□
8		200 μm × 200 μm	5 μm	Al/PET	60 ± 15 Ω/□ (91%) /73 ± 10 Ω/□
9		100 μm × 100 μm	10 μm	Cu/PET	8 ± 3 Ω/□ (79%) /10 ± 3 Ω/□
10		200 μm × 200 μm	5 μm	Cu/PET	30 ± 6 Ω/□ (91%) /30 ± 5 Ω/□
11	ITO			glass	30−80 Ω/□ (90%)
12	PEDOT/PSS[31]			glass/PET	100 Ω/□ (with 5% DMSO)(90%)
13	SWCNTs[32]			glass	150 Ω/□ (90%)
14	graphene[7]			glass	350 Ω/□ (90%)
15	graphene/SWCNTs[33]			glass	280 Ω/□ (86%)
16	silver nanowires[27]			PET	110 Ω/□ (90%)
17	graphene[24] (doped by $AuCl_3$)			glass	150 Ω/□ (87%)
18	graphene[25] (doped by $AuCl_3$)			PET	54 Ω/□ (85%)
19	graphene[23] (doped by HNO_3)			PET	30 Ω/□ (90%)

[a] The metal films on glass substrate were prepared by sputtering. The metal films on PET substrate were prepared by thermal evaporation. When gold was used as the metal grid material, a thin layer of titanium (5 nm) was used as adhesion layer. When copper was used as the metal grid material, a thin layer of aluminum (5 nm) was used as the adhesion layer. The thickness of the metal layer was 100 nm in all cases. The best results from published alternative transparent conducting electrode materials are in entries 11−19. [b] Transmission of hybrid film at 550 nm, excluding substrate absorption which was subtracted using a blank substrate.

high throughput method with which large substrates can be easily processed. Second, the metal grid networks formed by photolithography have minimal contact resistance between grid-lines. In randomly formed metal nanowire or carbon nanotube networks, the contact resistances are generally much larger than that of the single wire or tube, which make those films more resistive than expected. Furthermore, wet-etching is preferred over lift-off techniques since the former procedure has better yields on large devices. Other, more cost-effective techniques, such as inkjet or gravure printing of the metal nanowire or nanoparticle solution, are available for making the metal grid structure needed.

The graphene film was grown on copper either by using a gas carbon source[15] or solid carbon source.[30] The sheet resistance of the hybrid transparent electrode was measured by an Alessi four-point probe. The reported values are based on an average of 20 measurements for each sample. The sheet resistance of the metal grid electrode was determined using a two-terminal measurement on a square-shaped metal grid structure. The four-point probe was not used since the tips could not be landed on the metal areas. The transmittance was measured by a Shimadzu UV−vis−NIR spectrometer. The results are shown in Table 1.

As seen in Table 1, the graphene/metal grid hybrid transparent electrode can match or outperform all reported transparent electrode materials. The sheet resistance of the hybrid film was as low as 20 Ω/□ with transmittance over 90%; at lower transmittance (∼80%) the sheet resistance can reach 3 Ω/□. We also listed the sheet resistance of the grid-only structure, which is slightly higher than the hybrid structure. However, the grid-only structures have large empty spaces on the substrate and the four-point probe cannot measure the sheet resistance correctly because the tip of the probe lands on empty spaces. Instead, the resistance was measured by a two-terminal method with a flat contact electrode and the sheet resistance was calculated based on the resistance and the shape of the electrode. There might be some contact resistance with the two-terminal measurement. Compared to the metal grid-only structure, the hybrid electrode is a continuous conductive film and has advantages in the area where continuous transparent conductive films are required, such as in photovoltaic applications.

To evaluate the performance of the transparent conducting electrode, it is necessary to consider both sheet resistance and transmittance. Unfortunately literature sheet resistance data are often taken under different transmittance values, making direct comparisons difficult. Recently, a theoretical model for few-layer graphene has been proposed,[34] which gives the relationship between transmittance and sheet resistance. On the basis of the model of few-layered graphene, the transmittance and sheet resistance of graphene can be expressed by the following equation:

$$T = \left(1 + \frac{z_0}{2R_s}\frac{G_0}{G_{2D}}\right)^{-2} \quad (3)$$

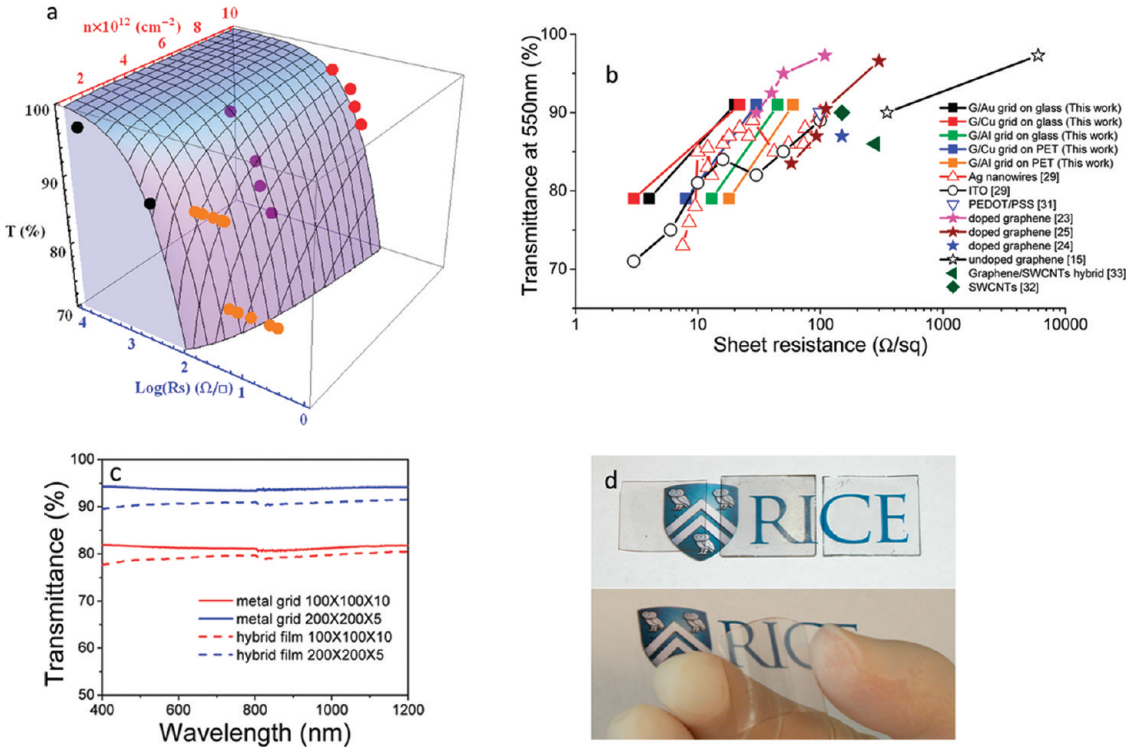

Figure 2. Analysis and comparison of transparent electrodes. (a) Transmittance (black axis), sheet resistance (blue axis), and charge carrier density (red axis) of graphene transparent electrodes. The mesh surface is the calculated relationship of transmittance to sheet resistance and carrier density based on eq 3, using a mobility of 5000 $cm^2 V^{-1} s^{-1}$. The orange dots are the hybrid graphene electrodes used in this work. They have carrier densities similar to undoped graphene, therefore they were placed in the plane with the smallest charge carrier density in the figure. The black dots are undoped CVD graphene,[15] on the same plane as hybrid graphene. The red dots are HNO_3-doped graphene,[23] which matched the calculated results very well. The purple dots are $AuCl_3$ doped graphene;[25] since their carrier density is not reported, the data points were placed midway between 10^{12} and 10^{13} cm^{-2}. (b) Transmittance and sheet resistances of the hybrid graphene electrodes compared to commercial transparent electrode materials and previous research results. (c) Transmittance of the metal grids and the hybrid film (100 × 100 × 10 (red lines): metal grid size is 100 μm × 100 μm and metal grid line width is 10 μm, 200 × 200 × 5 (blue lines): metal grid size is 200 μm × 200 μm and metal grid line width is 5 μm (see Supporting Information Table S1 for detail)). The theoretical transmittance of the metal grid frame can be calculated on the basis of the design (Supporting Information Table S1). (d) Photos of hybrid graphene films on glass and PET substrates. In the upper part of d, from left to right, are photos of the graphene/copper grid hybrid (200 × 200 × 5) electrode on PET; the graphene/gold grid hybrid (100 × 100 × 10) electrode on glass; and the graphene/copper grid hybrid (100 × 100 × 10) electrode on glass, respectively. The bottom photo is a bent graphene/copper grid hybrid electrode on PET. Panel d reprinted with permission from Rice University.

Where $Z_0 = 1/\varepsilon_0 c = 377\ \Omega$ is the free-space impedance, ε_0 is the free-space electric constant and c is the speed of light. $G_0 = 1.5e^2/(4\hbar) \approx 9.12 \times 10^{-5}\ \Omega^{-1}$ is the optical conductivity.[35] In graphene, the bidimensional d.c. conductivity $\sigma_{2D} = n\mu e$, where n is the number of charge carriers and μ is the mobility. In general semiconductors, the mobility drops when the charge carrier density increases. However, experimental results show that the mobility of graphene is not affected by chemically induced ionized impurities in the graphene in concentrations as high as 10^{12} cm^{-2} (where the dopants are less than 10 nm apart) until it reaches values of $\sim 10^5$ $cm^2 \cdot V^{-1} \cdot s^{-1}$.[36,37] At higher carrier concentration, the mobility of graphene can be affected. For example, when the carrier density reaches 10^{13} cm^{-2}, the experimental observed mobility of graphene is between 2000 and 10000 $cm^2 \cdot V^{-1} \cdot s^{-1}$.[20,36] As long as the graphene transparent electrodes are made by a scalable method such as chemical vapor deposition, they can reach mobilities of 4000−5000 $cm^2 \cdot V^{-1} \cdot s^{-1}$ at room temperature when placed on an insulating substrate. We assume chemical doping will not change this mobility when the carrier density is smaller than 10^{13} cm^{-2}.

On the basis of eq 3, the sheet resistance and transmittance of graphene are plotted in Figure 2a. The mesh surface in Figure 2a could be regarded as the limitation of the present graphene transparent electrode (according to the mobility of 5000 $cm^2 V^{-1} s^{-1}$) and the shadowed region under the surface is achievable by present graphene transparent electrodes. The previously reported graphene transparent electrode data is plotted in Figure 2a as well (also available from Supporting Information Figure S12), The most heavily doped material results[23] (red dots in Figure 2a) slightly exceed the calculation limit. Other undoped[15] (black dots in Figure 2a) or doped graphene[25] (purple dots in Figure 2a) show sheet resistances larger than the theoretical limit at the same transmittance (in the shadow region). In the hybrid electrode of this work, the graphene is not doped. Hence, we assume that they have similar carrier densities to pristine graphene,

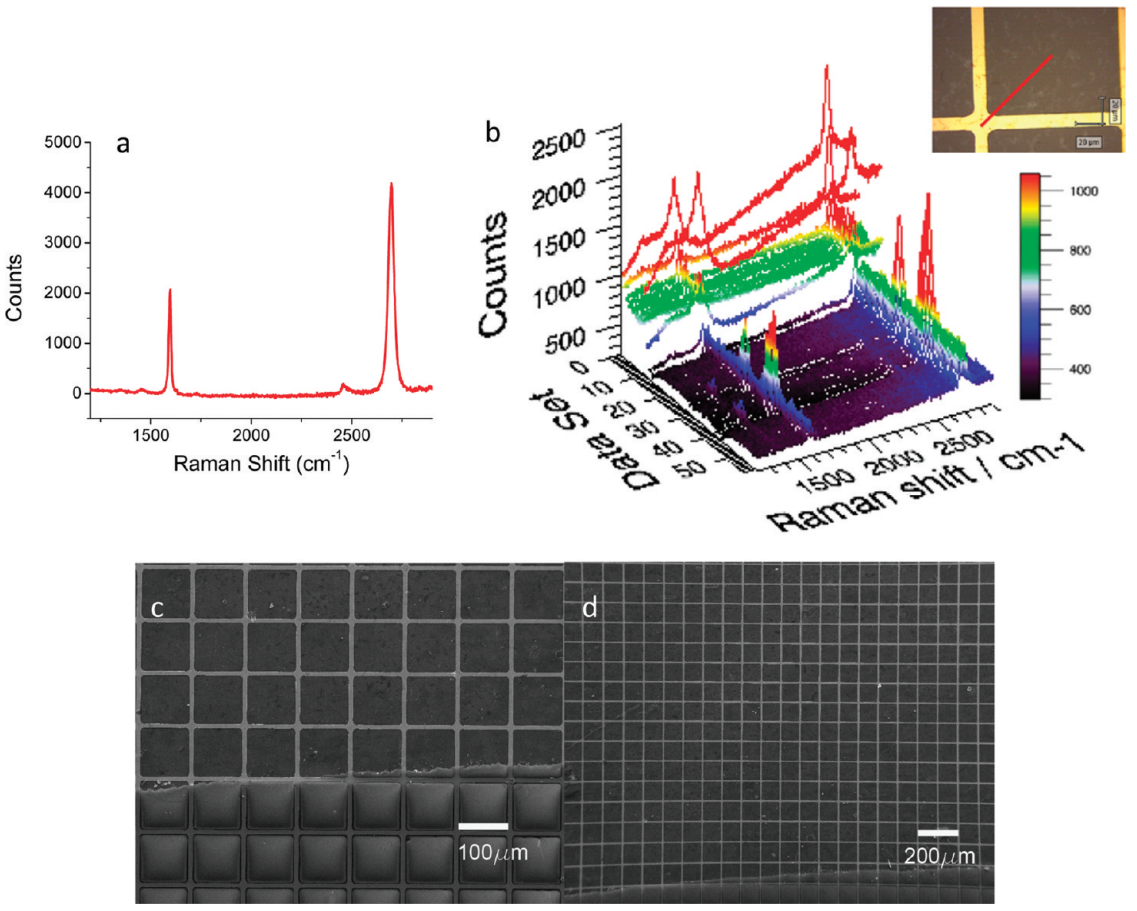

Figure 3. Spectroscopic and SEM analyses of materials in this work. (a) Raman spectrum of graphene used in this work. The spectrum was taken using transferred graphene on SiO_2 surface. (b) Raman spectra of the graphene while on the metal grid-covered glass. The inset image shows the path where the Raman spectra were taken. The scale bar in inset is 20 μm. (c) SEM images of the hybrid transparent electrode. Graphene covered areas are darker and flat.

which is $<10^{12}$ cm^{-2} at room temperature. It is clear that all hybrid electrode results in this work (orange dots in Figure 2a) outperformed the theoretical limit of present graphene (surface in Figure 2a). Considering the graphene used in this work has similar mobility as that from other reported scalable methods,[15,23,30] the highly conductive metal network underneath should also contribute to the low sheet resistance recorded. The gold or copper grid-based hybrid transparent electrodes show better performance than all reported graphene transparent electrodes. The lower efficiency of the graphene aluminum grid electrode might originate from the surface oxide on the aluminum causing a higher contact resistance.

The results of this work are also compared in Figure 2b with that of other types of transparent electrode. It is clear that the hybrid graphene transparent electrode is the best choice between the transmittance range of 70–91%, which is enough for most transparent conducting electrode-based applications.

The broad absorbance spectra of the graphene/metal grid hybrid film are plotted in Figure 2c. The transmittances of the hybrid film are almost flat in the range of 400–1200 nm, in contrast to ITO, which has a transmittance maximum at 550 nm. The additional graphene layer introduced the expected 2–3% loss of transmittance compared with the original metal grid frame. Furthermore, the hybrid film adapts to both rigid (glass) and flexible (PET) substrates (Figure 2d), rendering it a general purpose transparent conducting electrode material.

The graphene film used in this work was predominantly composed of a monolayer as analysis using Raman spectroscopy indicated (Figure 3a). When Raman spectra were taken directly from the hybrid electrode, the metal enhancement was observed where there was a metal line underneath. Full coverage of graphene on the grid structure was confirmed by Raman mapping (Figure 3b) and SEM images (Figure 3c). Figure 3c shows the edges of the graphene film, where the contrast between the graphene covered and noncovered grid is clear. More optical images are shown in the Supporting Information (Figure S7–S11).

The flexibility of the electrode was tested for the samples fabricated using PET substrates. The hybrid electrode was bent multiple times to radii of 5 mm (according to tensile strain ~3% when PET substrate thickness of 0.3 mm is counted). The results are shown in Figure 4b. The sheet resistances of the hybrid film increased 20%–30%; however, after the initial 50

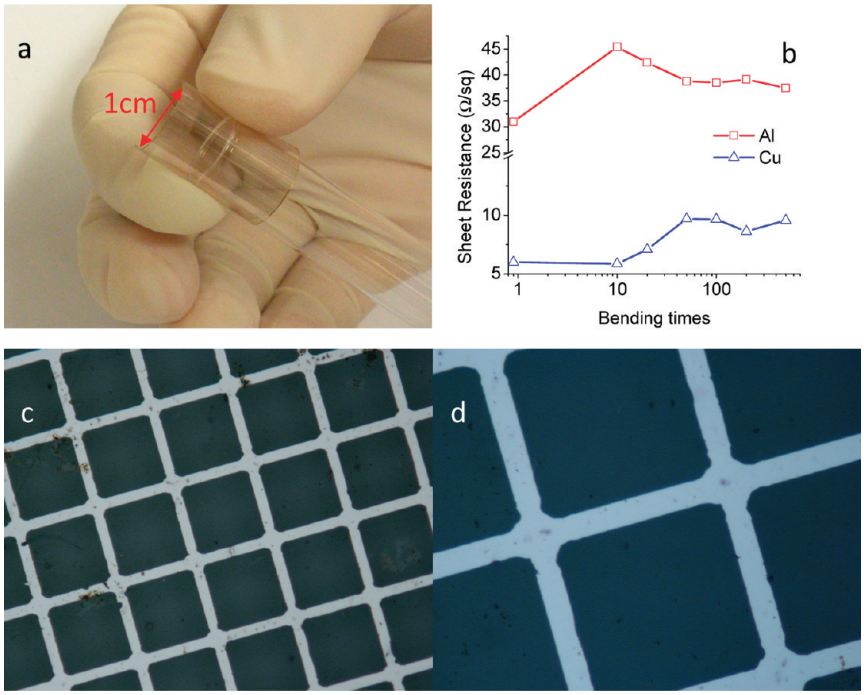

Figure 4. Flexibility test of the hybrid electrode fabricated on a PET surface. (a) Image of a bent hybrid electrode on the PET substrate. The electrode was bent to a $d = 1$ cm cylinder. (b) The sheet resistance of the hybrid electrode (100 × 100 × 10), as a function of bending cycles, up to 500 bending cycles. (c,d) optical images of the hybrid film structure after 500 bending cycles.

bending cycles, the sheet resistances stabilized and did not have significant variations up to 500 bending cycles. The initial change of the sheet resistance may originate from the graphene film itself, which was also observed from the pure graphene electrodes.[7] A possible explanation is that there are weak areas (such as grain boundaries or induced imperfections during the transferring process) on the graphene where the force is concentrated upon bending. Those areas might not survive at the bending angles tested and then change their form. After an initial number of cycles, all of those areas are stabilized and the sheet resistance becomes constant. The optical images in Figure 4c,d also indicate that there are no obvious cracks formed on the metal grid lines after the 500 bending cycles. The flexibility of the hybrid electrode is close to that of a recently published silver nanowire electrode.[27] Similar tests on an ITO PET electrode demonstrated an increase of sheet resistance over 2 orders of magnitude.[27] The pure graphene transparent electrode exhibits better flexibility, with a sheet resistance increase of 40% at tensile strain ~15%, however the better conductivity of the hybrid electrode could render it useful in several applications.

Another advantage of the hybrid electrode is that it uses nondoped graphene. Since no chemical doping was introduced to increase the carrier density of the graphene, the hybrid transparent electrodes are free of degradations originating from the dopant. The graphene/metal (including gold, copper, and aluminum) grid hybrid electrode was tested after exposure to ambient condition for 6 months and the sheet resistances were the same as the fresh samples; an indication of the stability of the electrode. Recent research shows that graphene acts as an oxidation resistance layer for metals and alloys,[38] giving further basis for optimism in the stability here.

In summary, a new graphene/metal grid hybrid transparent electrode has been developed. On the basis of the available data, the transparent metal grid/graphene electrode outperformed all commercial and research transparent conducting films in the transmittance range of 70−91%. The hybrid film is stable under ambient temperature when a suitable metal is used. The hybrid film can also be integrated onto a flexible substrate, which renders this hybrid film a general purpose transparent electrode material.

METHODS

Fabrication of metal grid: The glass slides were cut into 1 in. × 1 in. square samples by a dicing saw. The square samples were cleaned in a fresh piranha solution (7:3 mixture of 98% H_2SO_4/30% H_2O_2. Caution: The mixture is strongly oxidizing and may detonate upon contact with organic material), and then rinsed with deionized water. The cleaned samples were sputtered with 5 nm Ti and 100 nm Au using a CrC-150 sputter coater. Photoresist (Shipley 1813) was spun onto the Au film (4000 rpm, 60 s). The samples were baked and then exposed using the prepared grid mask. After being developed by MICROPOSIT MF-319 developer (45 s), the films were baked again on a hot-plate (110 °C) for 10 min. The second bake is

important to obtain defect-free grid structures on the inch-sized samples. The samples were then etched by the Au etchant and then the Ti etchant. The residual photoresist was removed with hot acetone (see Scheme S1 in Supporting Information for detailed information).

Assembly of hybrid electrodes: Graphene was grown using a recently developed low temperature growth technique with solid carbon source.[30] In some cases, the standard CVD method was applied as well.[15] The graphene used in this work had mobilities between 700 and 2000 $cm^2 V^{-1} s^{-1}$. The wet transfer technique[30] was used to transfer graphene onto the metal grid substrate. In brief, a thin layer of PMMA was spun on the graphene covered copper foil, and then the copper was etched with copper etchant. The floating PMMA passivated graphene was rinsed with water several times and transferred on various metal grid substrates. The sacrificial PMMA was finally removed with an acetone rinse at room temperature. The hybrid transparent electrode was dried in a vacuum oven overnight (see Supporting Information for detailed information).

Acknowledgment. The authors thank J. Yao for helpful discussions. The work was funded by the Office of Naval Research Graphene MURI program (00006766, N00014-09-1-1066), the Air Force Research Laboratory through University Technology Corporation (09-S568-064-01-C1), the Air Force Office of Scientific Research (FA9550-09-1-0581), and the Lockheed Martin Corporation through the LANCER IV Program.

Supporting Information Available: Experimental procedures, optical images of graphene and hybrid transparent electrodes. This material is available free of charge *via* the Internet at http://pubs.acs.org.

REFERENCES AND NOTES

1. Becerril, H. c. A.; Mao, J.; Liu, Z.; Stoltenberg, R. M.; Bao, Z.; Chen, Y. Evaluation of Solution-Processed Reduced Graphene Oxide Films as Transparent Conductors. *ACS Nano* **2008**, *2*, 463–470.
2. Dan, B.; Irvin, G. C.; Pasquali, M. Continuous and Scalable Fabrication of Transparent Conducting Carbon Nanotube Films. *ACS Nano* **2009**, *3*, 835–843.
3. Eda, G.; Lin, Y. Y.; Miller, S.; Chen, C. W.; Su, W. F.; Chhowalla, M. Transparent and Conducting Electrodes for Organic Electronics from Reduced Graphene Oxide. *Appl. Phys. Lett.* **2008**, *92*, 233305.
4. Wu, J. B.; Becerril, H. A.; Bao, Z. N.; Liu, Z. F.; Chen, Y. S.; Peumans, P. Organic Solar Cells with Solution-Processed Graphene Transparent Electrodes. *Appl. Phys. Lett.* **2008**, *92*, 263302.
5. Zhu, Y. W.; Cai, W. W.; Piner, R. D.; Velamakanni, A.; Ruoff, R. S. Transparent Self-Assembled Films of Reduced Graphene Oxide Platelets. *Appl. Phys. Lett.* **2009**, *95*, 103104.
6. Blake, P.; Brimicombe, P. D.; Nair, R. R.; Booth, T. J.; Jiang, D.; Schedin, F.; Ponomarenko, L. A.; Morozov, S. V.; Gleeson, H. F.; Hill, E. W.; *et al*. Graphene-Based Liquid Crystal Device. *Nano Lett.* **2008**, *8*, 1704–1708.
7. Li, X.; Zhu, Y.; Cai, W.; Borysiak, M.; Han, B.; Chen, D.; Piner, R. D.; Colombo, L.; Ruoff, R. S. Transfer of Large-Area Graphene Films for High-Performance Transparent Conductive Electrodes. *Nano Lett.* **2009**, *9*, 4359–4363.
8. Reina, A.; Jia, X.; Ho, J.; Nezich, D.; Son, H.; Bulovic, V.; Dresselhaus, M. S.; Kong, J. Large Area, Few-Layer Graphene Films on Arbitrary Substrates by Chemical Vapor Deposition. *Nano Lett.* **2008**, *9*, 30–35.
9. Wang, X.; Zhi, L.; Mullen, K. Transparent, Conductive Graphene Electrodes for Dye-Sensitized Solar Cells. *Nano Lett.* **2007**, *8*, 323–327.
10. Kim, K. S.; Zhao, Y.; Jang, H.; Lee, S. Y.; Kim, J. M.; Kim, K. S.; Ahn, J. H.; Kim, P.; Choi, J. Y.; Hong, B. H. Large-Scale Pattern Growth of Graphene Films for Stretchable Transparent Electrodes. *Nature* **2009**, *457*, 706–710.
11. Novoselov, K. S.; Geim, A. K.; Morozov, S. V.; Jiang, D.; Katsnelson, M. I.; Grigorieva, I. V.; Dubonos, S. V.; Firsov, A. A. Two-Dimensional Gas of Massless Dirac Fermions in Graphene. *Nature* **2005**, *438*, 197–200.
12. Zhang, Y. B.; Tan, Y. W.; Stormer, H. L.; Kim, P. Experimental Observation of the Quantum Hall Effect and Berry's Phase in Graphene. *Nature* **2005**, *438*, 201–204.
13. Li, X.; Zhang, G.; Bai, X.; Sun, X.; Wang, X.; Wang, E.; Dai, H. Highly Conducting Graphene Sheets and Langmuir–Blodgett Films. *Nat. Nanotechnol.* **2008**, *3*, 538–542.
14. Geim, A. K. Graphene: Status and Prospects. *Science* **2009**, *324*, 1530–1534.
15. Li, X.; Cai, W.; An, J.; Kim, S.; Nah, J.; Yang, D.; Piner, R.; Velamakanni, A.; Jung, I.; Tutuc, E.; *et al*. Large-Area Synthesis of High-Quality and Uniform Graphene Films on Copper Foils. *Science* **2009**, *324*, 1312–1314.
16. Nair, R. R.; Blake, P.; Grigorenko, A. N.; Novoselov, K. S.; Booth, T. J.; Stauber, T.; Peres, N. M. R.; Geim, A. K. Fine Structure Constant Defines Visual Transparency of Graphene. *Science* **2008**, *320*, 1308.
17. Bolotin, K. I.; Sikes, K. J.; Jiang, Z.; Klima, M.; Fudenberg, G.; Hone, J.; Kim, P.; Stormer, H. L. Ultrahigh Electron Mobility in Suspended Graphene. *Solid State Commun.* **2008**, *146*, 351–355.
18. Chen, J.-H.; Jang, C.; Xiao, S.; Ishigami, M.; Fuhrer, M. S. Intrinsic and Extrinsic Performance Limits of Graphene Devices on SiO_2. *Nat. Nanotechnol.* **2008**, *3*, 206–209.
19. Sze, S. M., *Semiconductor Devices: Physics and Technology*; Wiley: New York, 2001.
20. Novoselov, K. S.; Geim, A. K.; Morozov, S. V.; Jiang, D.; Zhang, Y.; Dubonos, S. V.; Grigorieva, I. V.; Firsov, A. A. Electric Field Effect in Atomically Thin Carbon Films. *Science* **2004**, *306*, 666–669.
21. Emtsev, K. V.; Bostwick, A.; Horn, K.; Jobst, J.; Kellogg, G. L.; Ley, L.; McChesney, J. L.; Ohta, T.; Reshanov, S. A.; Rohrl, J.; *et al*. Towards Wafer-Size Graphene Layers by Atmospheric Pressure Graphitization of Silicon Carbide. *Nat. Mater.* **2009**, *8*, 203–207.
22. Yu, Q. K.; Lian, J.; Siriponglert, S.; Li, H.; Chen, Y. P.; Pei, S. S. Graphene Segregated on Ni Surfaces and Transferred to Insulators. *Appl. Phys. Lett.* **2008**, *93*, 113103.
23. Bae, S.; Kim, H.; Lee, Y.; Xu, X.; Park, J.-S.; Zheng, Y.; Balakrishnan, J.; Lei, T.; Ri Kim, H.; Song, Y. I.; *et al*. Roll-to-Roll Production of 30-Inch Graphene Films for Transparent Electrodes. *Nat. Nanotechnol.* **2010**, *5*, 574–578.
24. Kim, K. K.; Reina, A.; Shi, Y.; Park, H.; Li, L.-J.; Lee, Y. H.; Kong, J. Enhancing the Conductivity of Transparent Graphene Films *via* Doping. *Nanotechnology* **2010**, *21*, 285205.
25. Güneş, F.; Shin, H.-J.; Biswas, C.; Han, G. H.; Kim, E. S.; Chae, S. J.; Choi, J.-Y.; Lee, Y. H. Layer-by-Layer Doping of Few-Layer Graphene Film. *ACS Nano* **2010**, *4*, 4595–4600.
26. Jackson, R.; Domercq, B.; Jain, R.; Kippelen, B.; Graham, S. Stability of Doped Transparent Carbon Nanotube Electrodes. *Adv. Funct. Mater.* **2008**, *18*, 2548–2554.
27. Hu, L.; Kim, H. S.; Lee, J.-Y.; Peumans, P.; Cui, Y. Scalable Coating and Properties of Transparent, Flexible, Silver Nanowire Electrodes. *ACS Nano* **2010**, *4*, 2955–2963.
28. De, S.; Higgins, T. M.; Lyons, P. E.; Doherty, E. M.; Nirmalraj, P. N.; Blau, W. J.; Boland, J. J.; Coleman, J. N. Silver Nanowire Networks as Flexible, Transparent, Conducting Films: Extremely High DC to Optical Conductivity Ratios. *ACS Nano* **2009**, *3*, 1767–1774.
29. Lee, J. Y.; Connor, S. T.; Cui, Y.; Peumans, P. Solution-Processed Metal Nanowire Mesh Transparent Electrodes. *Nano Lett.* **2008**, *8*, 689–692.
30. Sun, Z.; Yan, Z.; Yao, J.; Beitler, E.; Zhu, Y.; Tour, J. M. Growth of Graphene from Solid Carbon Sources. *Nature* **2010**, *468*, 549–552.
31. Starck, H. C. http://www.clevios.com, (accessed July 25, 2011).
32. Geng, H.-Z.; Kim, K. K.; So, K. P.; Lee, Y. S.; Chang, Y.; Lee, Y. H. Effect of Acid Treatment on Carbon Nanotube-Based Flexible Transparent Conducting Films. *J. Am. Chem. Soc.* **2007**, *129*, 7758–7759.
33. Tung, V. C.; Chen, L.-M.; Allen, M. J.; Wassei, J. K.; Nelson, K.; Kaner, R. B.; Yang, Y. Low-Temperature Solution Processing of Graphene–Carbon Nanotube Hybrid Materials for High-Performance Transparent Conductors. *Nano Lett.* **2009**, *9*, 1949–1955.

34. Bonaccorso, F.; Sun, Z.; Hasan, T.; Ferrari, A. C. Graphene Photonics and Optoelectronics. *Nat. Photon* **2010**, *4*, 611–622.
35. Mak, K. F.; Shan, J.; Heinz, T. F. Seeing Many-Body Effects in Single- and Few-Layer Graphene: Observation of Two-Dimensional Saddle-Point Excitons. *Phys. Rev. Lett.* **2011**, *106*, 046401.
36. Schedin, F.; Geim, A. K.; Morozov, S. V.; Hill, E. W.; Blake, P.; Katsnelson, M. I.; Novoselov, K. S. Detection of Individual Gas Molecules Adsorbed on Graphene. *Nat. Mater.* **2007**, *6*, 652–655.
37. Geim, A. K.; Novoselov, K. S. The Rise of Graphene. *Nat. Mater.* **2007**, *6*, 183–191.
38. Chen, S.; Brown, L.; Levendorf, M.; Cai, W.; Ju, S.-Y.; Edgeworth, J.; Li, X.; Magnuson, C. W.; Velamakanni, A.; Piner, R. D.; *et al.* Oxidation Resistance of Graphene-Coated Cu and Cu/Ni Alloy. *ACS Nano* **2011**, *5*, 1321–1327.